Changes of mRNA expression underlying orbital adipogenesis in thyroid-associated orbitopathy

Xiao Jing Bai[1,2,3], Xiao Jing Chu[2], Tao Yang[4], Bo Ding Tong[1,3], Xin Qi[1,3], Yang Yang Peng[1,3], Yuan Li[1,3], Lu Jue Wang[1,3], Yun Ping Li[1,3]

[1]Department of Ophthalmology, the Second Xiangya Hospital of Central South University, Changsha, Hunan Province, China
[2]Department of Ophthalmology, the Aier Eye Hospital of Shanxi Province, Taiyuan, Shanxi Province, China
[3]Hunan Clinical Research Center of Ophthalmic Disease, Changsha, Hunan Province, China
[4]College of Life Sciences, South China Agricultural University, Guangzhou, Guangdong Province, China

Corresponding author:
Yun Ping Li
Department of Ophthalmology
the Second Xiangya Hospital
Central South University
Changsha 410011
Hunan Province, China
E-mail: amyli@csu.edu.cn

Thyroid-associated orbitopathy (TAO), also known as Graves' ophthalmopathy, is the most common orbital disease in adults. It is the most prevalent extrathyroidal manifestation of Graves' disease, affecting up to 50% of the patients [1]. TAO is an autoimmune disorder characterized by immune-mediated inflammation of the adipose tissue and extraocular muscles, and clinically manifests as proptosis and double and/or impaired vision (Figure 1). This can cause permanent facial disfigurement and even blindness [2]. The monoclonal antibody teprotumumab, which targets the insulin-like growth factor 1 receptor (IGF-1R), has shown unprecedented clinical potential for TAO treatment [3]. However, a large proportion of patients with TAO at the inactive stage are refractory to therapy. In addition to surgical treatment, limited non-invasive and effective therapeutic options are available for these patients. Thus, a better understanding of the pathophysiology of patients with inactive TAO could provide insights for developing new therapeutic targets that may better help the patients for whom the current medication is ineffective.

Remodeling of the orbital connective tissue including hyperplasia of fat tissue, fibrosis of extraocular muscles and accumulation of glycosaminoglycans is a feature of inactive TAO [2]. Orbital fibroblasts (OFs) are the key effectors in TAO pathogenesis. Transcriptomic profiling analysis of the orbital adipose tissue, OFs, and orbital adipose-derived stem cells (OASC) has highlighted the importance of immune and inflammatory responses during orbital adipogenesis [4], suggesting that *TIMD4*, *DEFA1*, *DEFA1B*, and *DEFA3* may be involved in the innate immune-mediated orbital inflammation in TAO [4]. Moreover, elevated expression levels of secreted frizzled-related protein-1 (*sFRP-1*) and cysteine-rich, angiogenic inducer, 61 (*CYR61*) as well as downregulated expression of parathyroid hormone-like hormone (*PTHLH*) may stimulate orbital adipose tissue expansion [4–7]. However, further studies are required to elucidate the molecular mechanisms underlying the complex pathogenesis of TAO. Therefore, in this study, we investigated the transcriptional reprogramming in the orbital tissue of patients with TAO and explored potential therapeutic targets for the treatment of inactive TAO.

AMS
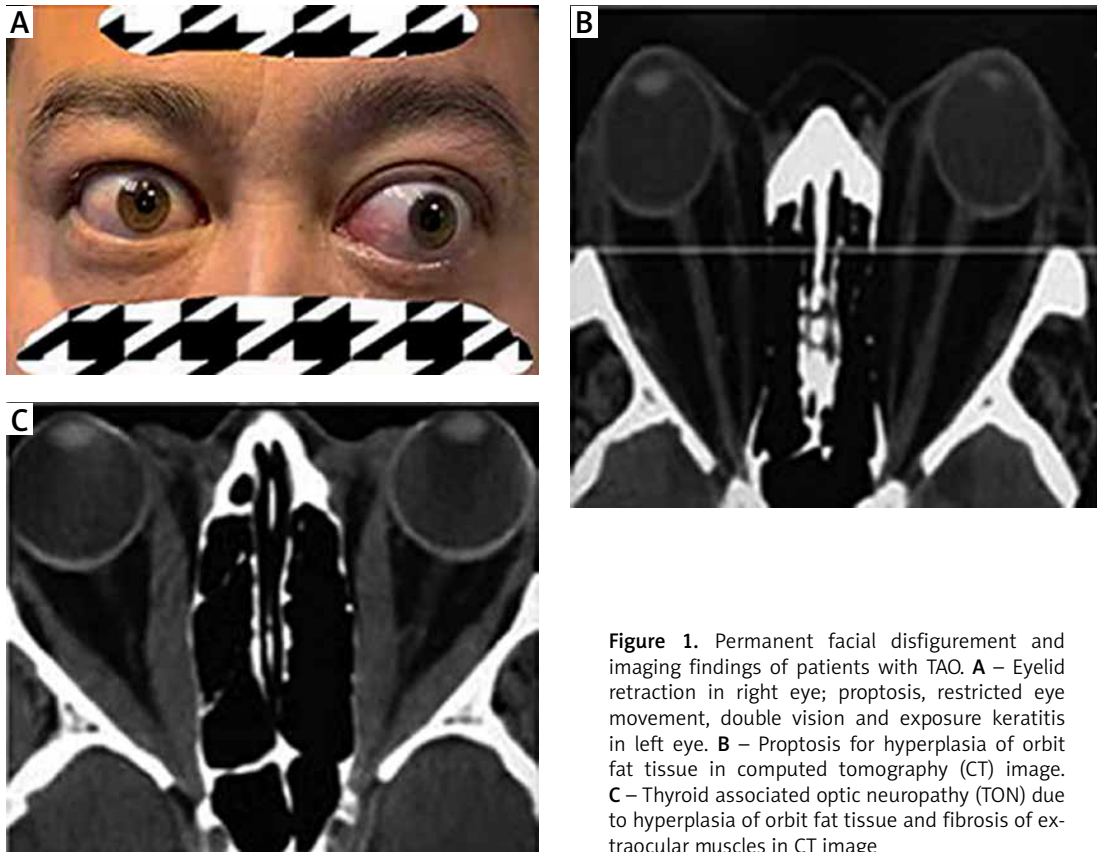
Figure 1. Permanent facial disfigurement and imaging findings of patients with TAO. **A** – Eyelid retraction in right eye; proptosis, restricted eye movement, double vision and exposure keratitis in left eye. **B** – Proptosis for hyperplasia of orbit fat tissue in computed tomography (CT) image. **C** – Thyroid associated optic neuropathy (TON) due to hyperplasia of orbit fat tissue and fibrosis of extraocular muscles in CT image

All patients enrolled in this study were diagnosed with TAO based on the guidelines of the European Thyroid Association/European Group on Graves's Orbitopathy (2016EUGOGO [8]). Patients with cancer, other autoimmune diseases or elevated IgG4 levels in serum [9] were excluded from the study. Six euthyroid patients with TAO refractory to medical therapy, with a clinical activity score (CAS) of less than 3 for at least 6 months, were selected as research subjects. Six control samples were acquired from the post-orbital septal adipose tissue of patients without hyperthyroidism or other autoimmune diseases who had undergone cosmetic surgery. The basic characteristics of the participants included in this study are shown in Table I. After isolation, samples were quickly placed in

Table I. Clinical features of patients with TAO and controls for RNA-seq analysis

Sample n	Gender	Age [year][†]	DTED [month]	ET [mm]***	PT	CAS (0–7)****	Surgery
T1	F	36	48	19	Me + Mp	1	EdP
T2	M	20	12	26	Mp	1	EdP
T3	F	42	22	21	Me + Mp	2	EdP
T4	F	48	24	19	Me + Mp	1	EdP
T5	M	53	8	17	Mp	2	EdP
T6	M	17	24	21	Me + Mp	1	EdP
C1	F	30	–	≤ 14	–	0	blp
C2	F	23	–	≤ 14	–	0	blp
C3	F	20	–	≤ 14	–	0	blp
C4	F	28	–	≤ 14	–	0	blp
C5	F	23	–	≤ 14	–	0	blp
C6	F	50	–	≤ 14	–	0	Eof

*Me – methimazole, Blp – blepharoplasty, Edp – orbital decompression, DTED – duration of thyroid disease prior to surgery, ET – Hertel exophthalmometer, PT – previous treatment, Mp – methylprednisolonem, CAS – Clinical Activity Score, Eof – excision of orbital fat prolapsed, [†]p = 0.3719, ***p < 0.0001.*

cryotubes and stored in liquid nitrogen for short-term storage. For further experiments, the samples were transferred to a –80°C refrigerator and extracted within 24 h.

This study was approved by the Ethics Committee of the Second Xiang Ya Hospital of Central South University (No: 2021111) and conducted based on the principles of the Declaration of Helsinki. All patients signed an informed consent form in full awareness before enrollment.

Total RNA was extracted and isolated from each sample using TRIzol reagent (Invitrogen, Carlsbad, CA, USA), according to the manufacturer's protocol. RNA concentration and integrity were detected using Nanodrop 2000 (Thermo Scientific, Waltham, MA, USA) and an Agilent 2100 Bioanalyzer (Agilent Technologies, Palo Alto, CA, USA). All mRNA samples met the following criteria: optical density (OD) 260/280 = 1.8–2.2, RNA 28S/18S ≥ 1.0, and RNA integrity number ≥ 7.

Next, total mRNA was purified using oligo(dT)-attached magnetic beads and transformed into cDNA. Subsequently, the synthesized cDNAs were subjected to end-repair and then adenylated at the 3′ ends. The adenylated cDNA fragments were linked to adapters, amplified using PCR, and purified using Ampure XP Beads (AGENCOURT, Beverly, MA, USA). The library was evaluated using an Agilent 2100 Bioanalyzer for quality control. The resultant products were heated, denatured, and circularized by the splint oligo sequence to obtain a single-strand circle DNA (ssCir DNA) as the final library. The final library was amplified using phi29 (Thermo Fisher Scientific, MA, USA) to create DNA nanoballs (DNBs), which contained more than 300 copies of each molecule. DNBs were loaded into a patterned nanoarray and pair-end 150 bp reads were generated on the MGI2000 platform (BGI, Shenzhen, China).

Raw data containing sequencing adapters or low-quality sequences were filtered using the quality control software SOAPnuke (BGI, Shenzhen, China). After filtering, the number of reads per sample ranged from 36 to 48 million (M). These clean reads were aligned to the human reference genome (GRCh38) using HISAT2 (version 2.2.1) [10]. HTSeq (version 0.13.5) [11] was applied to the BAM files to calculate the counts mapped to each gene in the union-counting mode.

Raw read counts were provided as inputs to DESeq2 for differential expression analysis [12]. After excluding genes with less than ten total read counts or zero read counts in more than three samples, internal variance stabilizing transformation was used to normalize the count data. Genes with a $p < 0.05$ (adjusted by the Benjamini and Hochberg correction) and fold change > 2.0 were defined as differentially expressed genes. WebGestalt [13] was used to probe enriched terms and pathways using Gene Ontology (GO), Kyoto Encyclopedia of Genes and Genomes (KEGG), and Reactome databases. A significance level of FDR < 0.05 was applied.

Another 8 pairs of samples of patients with TAO and controls were analyzed by performing quantitative real-time reverse transcription (qRT-PCR). Total RNA was isolated from the orbital fat tissue using TRIzol reagent (Invitrogen, Carlsbad, CA, USA). mRNA was reverse-transcribed into cDNA using Oligo(dT) and RevertAid First Strand cDNA Synthesis Kit (Thermo Scientific, Waltham, MA, USA). qRT-PCR was performed and the results were analyzed using FastStart Universal SYBR Green Master (Rox) (Roche Diagnostics, Germany) in a StepOne Real-time PCR System (Applied Biosystems). β-actin was used as an endogenous control for normalization. The primers used for the qRT-PCR are listed in Table II. Relative gene expression data were analyzed using the comparative CT method.

The statistical significance of differences was assessed by Student's *t*-test. Differentially expressed RNAs were identified by fold change (FC) ≥ 2.0 and $p < 0.05$.

In this study, we identified 468 significant DEGs, with 245 DEGs having downregulated and 223 DEGs having upregulated expression, in TAO

Table II. Sequence of primers of genes for qRT-PCR

Gene name	Forward and reverse primer
WNT	F:5′GAGAAACGGCGTTTATCTTCG 3′
	R:5′ GGATTCGATGGAACCTTCTGAG 3′
WNT2	F:5′ TCTTGAAACAAGAGTGCAAGTG 3′
	R :5′TACACGAGGTCATTTTTCGTTG 3′
WNT4	F:5′ GAACCTGGAAGTCATGGACTC 3′
	R:5′ GTTAGACTTGCTGCTGAGTCTA 3′
PPARG	F :5′AGATCATTTACACAATGCTGGC 3′
	R :5′TAAAGTCACCAAAAGGCTTTCG 3′
FABP4	F :5′GGCCAAACCTAACATGATCATC 3′
	R :5′TTATGGTGCTCTTGACTTTCCT 3′
CXCR2	F:5′ AAGGTGAATGGCTGGATTTTTG 3′
	R :5′CCCAGATGCTGAGACATATGAA 3′
SCD	F:5′ CTTTCTGATCATTGCCAACACA 3′
	R:5′ TGTTTCTGAAAACTTGTGGTGG 3′
COL12A1	F:5′ CATTTGTTTGTGAAACTGCCAC 3′
	R:5′ ACGCATTCTTCTGAATCCTGTA 3′
C5	F:5′ GAGCGTTGTCCCAGTATTCTAT 3′
	R :5′ACACACTGTAAGAGTAGTCAGC 3′
C6	F :5′GACGAAGAAATGAAAGAGGTCG 3′
	R :5′CCAACAGTTTCAAAGCCAGTAA 3′
β-actin	F :5′AAAGACCTGTACGCCAACAC 3′
	R :5′GTCATACTCCTGCTTGCTGAT 3′
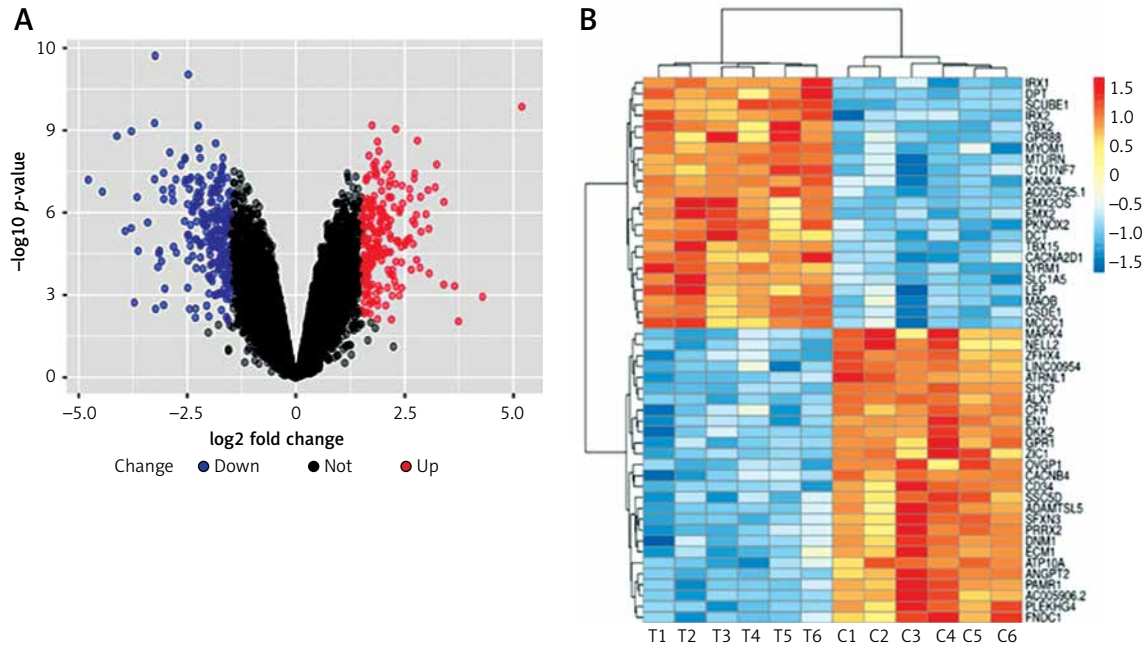
Figure 2. Differentially expressed genes of mRNA between patients with TAO and controls. **A** – The volcano plots display the fold-changes and *p*-values of differential mRNA expression in patients with TAO. Based on the relationship between fold-change and statistical significance, subsets of mRNAs were isolated. The cut-off for logFC is 1.5. The red point represents the upregulated mRNAs with statistical significance *p* < 0.05, while the blue point represents the significantly downregulated expression. **B** – The heatmap of the top 50 differentially expressed mRNAs in patients with TAO. Each row represents the relative expression level of an mRNA, and each column displays the expression level of a patient sample. Colors represent relative intensity of each sample. Red, high relative expression; blue, low relative expression

samples compared with that in controls, which were believed to contribute to TAO pathogenesis (FC ≥ 2.0, *p* < 0.05, Figure 2 A). The top 50 significantly altered (both upregulated and downregulated) DEGs are shown in Figure 2 B.

All the 468 DEGs underwent GO enrichment analysis and KEGG pathway analysis. The main enriched biological processes (BP) are extracellular matrix organization and extracellular structure organization (Figure 3 A). The main enriched cellular components (CC) are extracellular matrix and collagen-containing (Figure 3 B). The main enriched molecular functions (MF) are sulfur compound binding and receptor regulator activity (Figure 3 C).
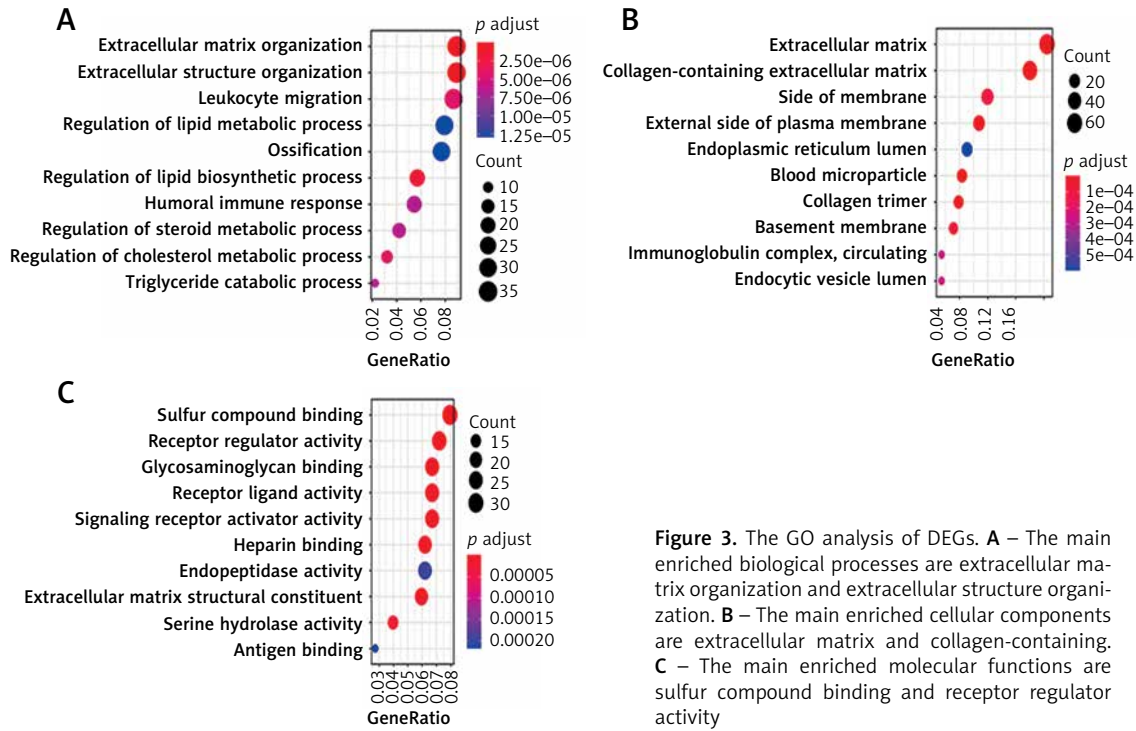
KEGG pathway analysis was conducted and demonstrated that the upregulated genes were involved in the PPAR signaling pathway, regulation of lipolysis in adipocytes, fatty acid metabolism, glycerolipid metabolism and the insulin signaling pathway, while downregulated genes were enriched in the pathways including ECM-receptor interaction, protein digestion and absorption, proteoglycans in cancer, basal cell carcinoma and focal adhesion (Figure 4).

Ten genes were selected for qRT-PCR validation. *C5, WNT4, COL12A1, WNT, WNT2, C6, CXCR2, FABP4, PPARG,* and *SCD* were selected to validate the altered DEGs in sequence analysis. The results

showed that the expression of *C5* was significantly increased in orbit fat from patients with TAO (*p* < 0.0001, Figure 5). Likewise, *COL12A1, WNT,* and *WNT4* were significantly decreased in orbit fat from patients with TAO (*p* < 0.01 and *p* < 0.05 respectively; Figure 5). The differential expression levels of *WNT2, C6, CXCR2, FABP4, PPARG* and *SCD* between the two groups were not statistically significant (Figure 5). The qRT-PCR results were consistent with the mRNA sequence.

Previous studies investigated transcriptomic profiling of TAO orbit fat from orbital fibroblasts undergoing adipogenesis or adipose-derived stem cells [4, 14]. By using next generation RNA sequencing technology, transcriptome analysis of orbital adipose tissue in active TAO was conducted [15]; however, the study did not involve the inactive ones. There were no effective treatments for those patients with TAO, especially with proptosis.

We validated the dysregulation of Wnt signaling and enhanced expression of complement genes in inactive TAO. Expression of genes involved in connective tissue development and collagen biosynthesis was also significantly altered in the TAO samples compared with that in the controls. These results highlight the importance of transcriptional and post-transcriptional regulatory processes in TAO pathogenesis.

Xiao Jing Bai, Xiao Jing Chu, Tao Yang, Bo Ding Tong, Xin Qi, Yang Yang Peng, Yuan Li, Lu Jue Wang, Yun Ping Li

Figure 3. The GO analysis of DEGs. **A** – The main enriched biological processes are extracellular matrix organization and extracellular structure organization. **B** – The main enriched cellular components are extracellular matrix and collagen-containing. **C** – The main enriched molecular functions are sulfur compound binding and receptor regulator activity
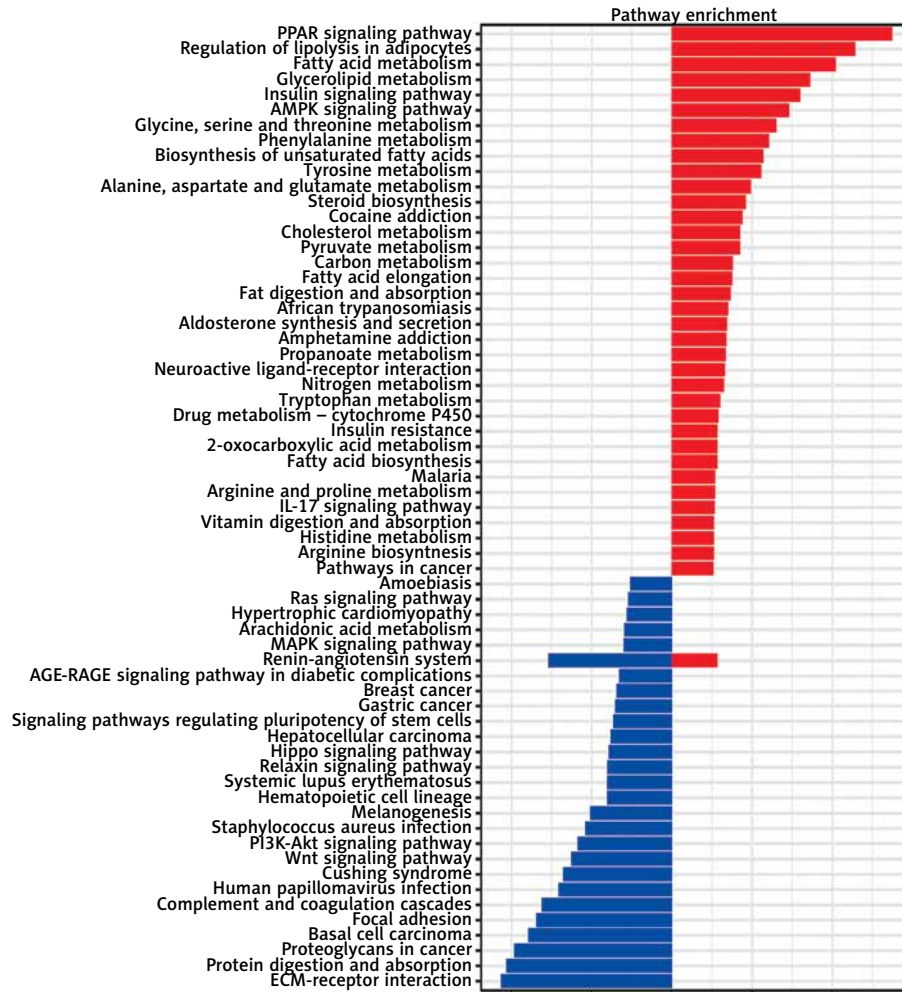
Figure 4. KEGG pathway analyses of DEGs. Red represents upregulated DEGs, while blue represents downregulated DEGs
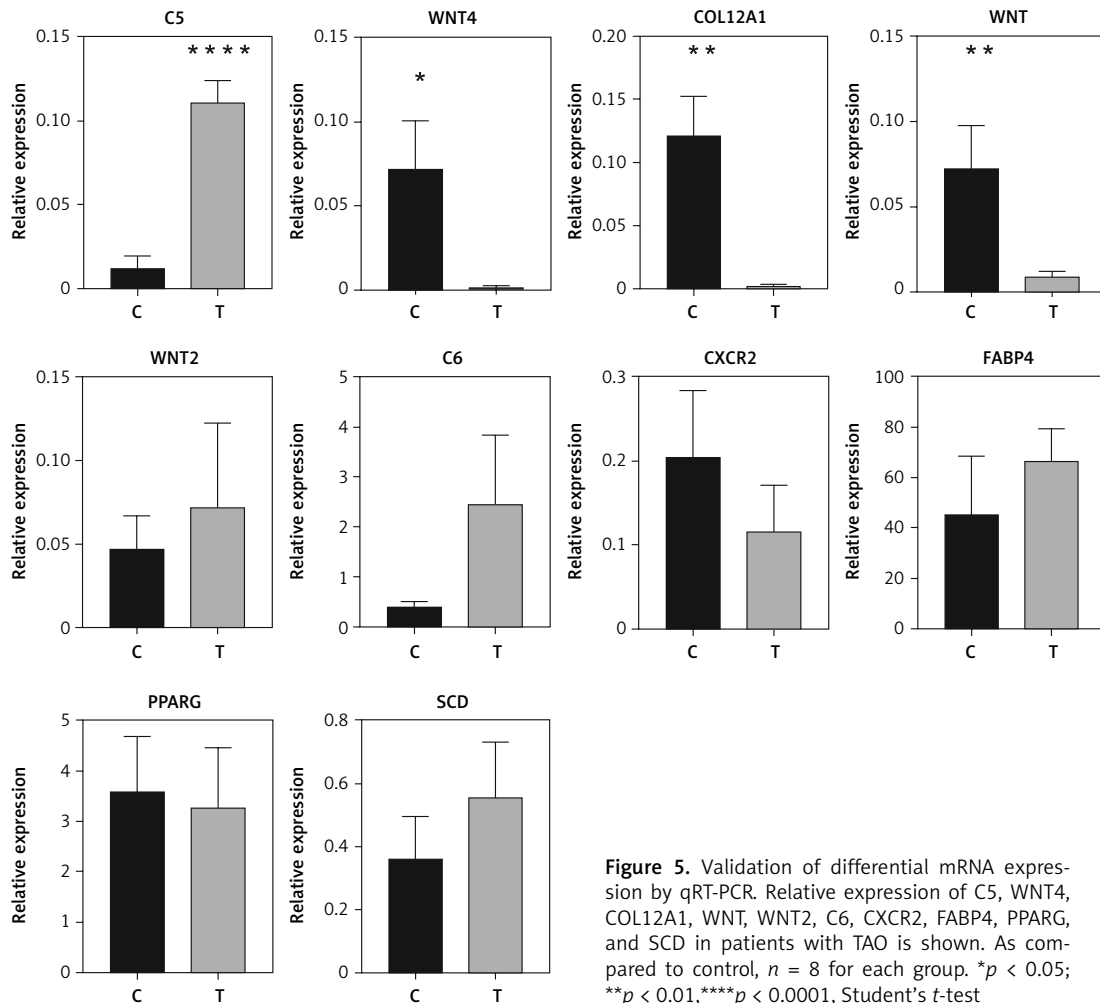
Figure 5. Validation of differential mRNA expression by qRT-PCR. Relative expression of C5, WNT4, COL12A1, WNT, WNT2, C6, CXCR2, FABP4, PPARG, and SCD in patients with TAO is shown. As compared to control, $n = 8$ for each group. *$p < 0.05$; **$p < 0.01$,****$p < 0.0001$, Student's t-test

Previous studies have demonstrated a connection between the Wnt signaling pathway and adipogenesis. Differential expression of *Wnt5A*, *sFRPs*, and *DKK* was observed in patients with TAO who were not subjected to anti-inflammatory treatment [16]. Even after eliminating the influence of inflammatory factors in the vitro experiment, the expression of Wnt signaling pathway components was significantly suppressed in OASCs [4]. During adipogenesis, *WNT5A* was overexpressed only during the early stage and the expression gradually decreases during the differentiation process [14]. Consistent with the results of previous studies, downregulation of *WNT* and *WNT4* expression was observed in TAO, even in patients who had received anti-inflammatory therapies. These results suggest that except for inflammatory factors, other unknown regulatory factors may inhibit the expression of Wnt signaling pathway genes in TAO, which should be investigated further.

Considering that autoimmune diseases may have similar underlying pathological processes, we speculated that elevated expression of *C5* in TAO may promote remodeling of the orbital tissue for the following reasons. First, *C5* is closely associated with inflammation. An autoimmune response can activate the complement system. Activated C5 (C5a) not only recruits inflammatory cells to induce inflammation but also enhances the expression of IL-17 to aggravate the inflammatory response [17, 18]. IL-17A can exacerbate fibrosis by promoting the proinflammatory and profibrotic function of OFs in TAO [19]. Furthermore, in the study, the expression of C5a receptor (C5aR) in adipose tissue was positively correlated with local inflammation, which could be reversed by the C5aR antagonist (C5aRa) in the mouse model [20]. This highlights the strong connection between *C5* expression and inflammation in adipose tissue. Second, C5, especially C5a, has been identified as a new profibrotic factor and a potential new therapeutic target because it can stimulate the production of TGF-β1. C5aRa can inhibit the production of TGF-β1 in cultured mouse renal tubular cells [21]. TGF-β1 is a key factor in promoting the differentiation of OFs into myofibroblasts, which leads to fibrosis of the extraocular muscle in TAO [22]. Elevated expression of C5a in an inflammatory environment promotes fibrosis in the kidneys [23]. Finally, *C5* has shown potential in the treat-

Xiao Jing Bai, Xiao Jing Chu, Tao Yang, Bo Ding Tong, Xin Qi, Yang Yang Peng, Yuan Li, Lu Jue Wang, Yun Ping Li

ment of autoimmune diseases. The humanized monoclonal antibody eculizumab against C5 can reduce the risk of optic neuritis spectrum disease recurrence and shows a better effect in a variety of refractory autoimmune diseases [24–26]. Furthermore, C5 expression was detected in the thyroid tissue of patients with Graves' disease via immunohistochemistry [27]. Therefore, *C5* may also play a crucial role in the development of TAO lesions and is a potential therapeutic target for TAO; however, further studies are required to determine the role of *C5*.

Changes in extracellular matrix components can influence the function of the cells residing in it [28]. The activated effector cells in TAO secrete large amounts of hyaluronic acid to remodel the extracellular matrix, which can affect the proliferation and differentiation of preadipocytes [29]. The downregulation of different *COL12A1* transcripts caused by alternative splicing was observed in the active TAO orbital fat [30]. Consistent with previous results, low expression of *COL12A1* in TAO was also detected in this study, although the samples were derived from patients in the stable phase. Changes in collagen microstructure can regulate fibroblast differentiation and fibrosis by altering cellular mechanical signals [31]. However, whether the change in collagen composition is involved in the remodeling of the TAO orbital connective tissue requires further confirmation.

Our study has some limitations. First, the small sample size may have affected the representativeness of the results. Second, the control samples were all from young and middle-aged women, which resulted in a sex-related bias in sample collection. This bias may be reflected in the differential expression of sex-related genes. Although TAO is more prevalent in females, severe TAO is relatively more common in males [32]; therefore, the results of differential expression analysis be skewed. In the future, we will include more male and elderly patients in the control group to further verify the representativeness of the DEGs.

In conclusion, we identified a large number of novel DEGs, which help us to better characterize the molecular mechanisms underlying TAO pathogenesis, and provided new therapeutic targets at the transcriptional and post-transcriptional levels. These data could be an important resource for future research on TAO and autoimmune diseases. Notably, based on the results of transcriptome analysis and subsequent confirmatory studies, we propose that the *C5* and Wnt signaling pathways may stimulate connective tissue remodeling in TAO.

The Wnt signaling pathway and C5 are potential therapeutic targets for TAO, which have value for further research. Our study sheds new light on the mechanisms underlying TAO pathogenesis.

Conflict of interest

The authors declare no conflict of interest.

References

1. Lazarus JH. Epidemiology of Graves' orbitopathy (GO) and relationship with thyroid disease. Best Pract Res Clin Endocrinol Metab 2012; 26: 273-9.
2. Bahn RS. Graves' ophthalmopathy. N Engl J Med 2010; 362: 726-38.
3. Piantanida E, Bartalena L Teprotumumab: a new avenue for the management of moderate-to-severe and active Graves' orbitopathy? J Endocrinol Invest 2017; 40: 885-7.
4. Tao W, Ayala-Haedo JA, Field MG, Pelaez D, Wester ST. RNA-sequencing gene expression profiling of orbital adipose-derived stem cell population implicate HOX genes and WNT signaling dysregulation in the pathogenesis of thyroid-associated orbitopathy. Invest Ophthalmol Vis Sci 2017; 58: 6146-58.
5. Planck T, Parikh H, Brorson H, et al. Gene expression in Graves' ophthalmopathy and arm lymphedema: similarities and differences. Thyroid 2011; 21: 663-74.
6. Lantz M, Vondrichova T, Parikh H, et al. Overexpression of immediate early genes in active Graves' ophthalmopathy. J Clin Endocrinol Metab 2005; 90: 4784-91.
7. Kumar S, Leontovich A, Coenen MJ, Bahn RS. Gene expression profiling of orbital adipose tissue from patients with Graves' ophthalmopathy: a potential role for secreted frizzled-related protein-1 in orbital adipogenesis. J Clin Endocrinol Metab 2005; 90: 4730-5.
8. Bartalena L, Baldeschi L, Boboridis K, et al. The 2016 European Thyroid Association/European Group on graves' orbitopathy guidelines for the management of graves' orbitopathy. Eur Thyroid J 2016; 5: 9-26.
9. Rzepecka A, Babińska A, Sworczak K. IgG4-related disease in endocrine practice. Arch Med Sci 2019; 15: 55-64.
10. Kim D, Paggi JM, Park C, Bennett C, Salzberg SL. Graph-based genome alignment and genotyping with HISAT2 and HISAT-genotype. Nat Biotechnol 2019; 37: 907-15.
11. Anders S, Pyl PT, Huber W. HTSeq: a Python framework to work with high-throughput sequencing data. Bioinformatics 2015; 31: 166-9.
12. Love MI, Huber W, Anders S. Moderated estimation of fold change and dispersion for RNA-seq data with DESeq2. Genome Biol 2014; 15: 550.
13. Liao Y, Wang J, Jaehnig EJ, Shi Z, Zhang B. WebGestalt 2019: gene set analysis toolkit with revamped UIs and APIs. Nucleic Acids Res 2019; 47: W199-205.
14. Kim DW, Taneja K, Hoang T, et al. Transcriptomic profiling of control and thyroid-associated orbitopathy (TAO) orbital fat and TAO orbital fibroblasts undergoing adipogenesis. Invest Ophthalmol Vis Sci 2021; 62: 24.
15. Lee BW, Kumar VB, Biswas P, et al. Transcriptome analysis of orbital adipose tissue in active thyroid eye dis-

ease using next generation RNA sequencing technology. Open Ophthalmol J 2018; 12: 41-52.

16. Ezra DG, Krell J, Rose GE, Bailly M, Stebbing J, Castellano L. Transcriptome-level microarray expression profiling implicates IGF-1 and Wnt signalling dysregulation in the pathogenesis of thyroid-associated orbitopathy. J Clin Pathol 2012; 65: 608-13.

17. Guo RF, Ward PA. Role of C5a in inflammatory responses. Annu Rev Immunol 2005; 23: 821-52.

18. Liu B, Wei L, Meyerle C, et al. Complement component C5a promotes expression of IL-22 and IL-17 from human T cells and its implication in age-related macular degeneration. J Transl Med 2011; 9: 111.

19. Fang S, Huang Y, Wang N, et al. Insights into local orbital immunity: evidence for the involvement of the Th17 cell pathway in thyroid-associated ophthalmopathy. J Clin Endocrinol Metab 2019; 104: 1697-711.

20. Lim J, Iyer A, Suen JY, et al. C5aR and C3aR antagonists each inhibit diet-induced obesity, metabolic dysfunction, and adipocyte and macrophage signaling. FASEB J 2013; 27: 822-31.

21. Boor P, Konieczny A, Villa L, et al. Complement C5 mediates experimental tubulointerstitial fibrosis. J Am Soc Nephrol 2007; 18: 1508-15.

22. Koumas L, Smith TJ, Feldon S, Blumberg N, Phipps RP. Thy-1 expression in human fibroblast subsets defines myofibroblastic or lipofibroblastic phenotypes. Am J Pathol 2003; 163: 1291-300.

23. Portilla D, Xavier S. Role of intracellular complement activation in kidney fibrosis. Br J Pharmacol 2021; 178: 2880-91.

24. Pittock SJ, Berthele A, Fujihara K, et al. Eculizumab in Aquaporin-4-positive neuromyelitis optica spectrum disorder. N Engl J Med 2019; 381: 614-25.

25. Misawa S, Kuwabara S, Sato Y, et al. Safety and efficacy of eculizumab in Guillain-Barré syndrome: a multicentre, double-blind, randomised phase 2 trial. Lancet Neurol 2018; 17: 519-29.

26. Dhillon S. Eculizumab: a review in generalized myasthenia gravis. Drugs 2018; 78: 367-76.

27. Kasajima T, Yamakawa M, Imai Y. Immunohistochemical study of intrathyroidal lymph follicles. Clin Immunol Immunopathol 1987; 43: 117-28.

28. Theocharis AD, Skandalis SS, Gialeli C, Karamanos NK. Extracellular matrix structure. Adv Drug Deliv Rev 2016; 97: 4-27.

29. Dik WA, Virakul S, van Steensel L. Current perspectives on the role of orbital fibroblasts in the pathogenesis of Graves' ophthalmopathy. Exp Eye Res 2016; 142: 83-91.

30. Wu L, Liang Y, Song N, et al. Differential expression and alternative splicing of transcripts in orbital adipose/connective tissue of thyroid-associated ophthalmopathy. Exp Biol Med 2021; 246: 1990-2006.

31. Seo BR, Chen X, Ling L, et al. Collagen microarchitecture mechanically controls myofibroblast differentiation. Proc Natl Acad Sci USA 2020; 117: 11387-98.

32. Smith TJ, Hegedüs L. Graves' disease. N Engl J Med 2016; 375: 1552-65.